Synthesis of SLN Nanoparticles Containing Naringenin Decorated with Folate-Conjugated Chitosan to Evaluate its Anticancer Effects

Wurood Al-Kariti¹, Ali B. Roomi², Hamed Amiri³, Hossein Javid^{3,4,5}, Mehdi Karimi-Shahri^{6,7}

¹Department of Biochemistry, Faculty of Converging Sciences and Technologies, Islamic Azad University, Tehran, Iran, ²Department of Medical Laboratory, College of Health and Medical Technology, National University of Science and Technology, Thi-Qar, Iraq, ³Department of Clinical Biochemistry, Faculty of Medicine, Mashhad University of Medical Sciences, Mashhad, Iran, ⁴Department of Medical Laboratory Sciences, Varastegan Institute for Medical Sciences, Mashhad, Iran, ⁵Surgical Oncology Research Center, Mashhad University of Medical Sciences, Mashhad, Iran, ⁶Department of Pathology, Faculty of Medicine, Gonabad University of Medical Sciences, Gonabad, Iran

Abstract

Background: Solid lipid nanoparticles (SLNs) have shown promise as nanocarriers for cancer therapy, with the ability to be surface-modified with ligands such as transferrin and folic acid(FA) for targeting specific receptors on cancer cells. Objective: This study aimed to encapsulate naringenin (NRG) in lipid nanoparticles and investigate the toxic effects of SLNs containing NRG compared to surface-modified nanoparticles with chitosan-folate and free drugs. Materials and Methods: Nanoparticles composed of SLN and NRG were coated with folate-chitosan, and their physical and chemical properties were evaluated using dynamic light scattering, Fourier transform infrared, and electron microscopy. Drug encapsulation and folate binding were measured using the spectrophotometric absorption method. The toxicity and inhibitory pathways in cancer cells were examined. Results: The results of this investigation revealed a higher toxic effect of chitosan-folate-coated nanoparticles on breast cancer cells, which may be attributed to the transfer and internalization of nanoparticles into breast cancer cells as they possess positive folate receptors. Evaluation of the effects of nanoparticles on angiogenesis using the chorioallantoic membrane method demonstrated a decrease in the average number and length of blood vessels, as well as a decrease in embryo height and weight. Increased expression of P53, decreased expression of nuclear factor kappa B, and the results of acridine orange/propidium iodide staining, along with an increased level of reactive oxygen species in cells treated with nanoparticles, confirmed the induction of apoptosis by nanoparticles. The antibacterial test results also confirmed the inhibitory effects of nanoparticles on various strains of bacteria. Conclusion: These findings highlight the potential of nanoparticle-based treatments in preclinical research and demonstrate their effectiveness in suppressing cancer cell activity and combating bacterial strains.

Keywords: Angiogenesis, apoptosis, breast cancer cells, CAM method, naringenin, reactive oxygen species

Introduction

Cancer is a growth disorder caused by abnormal cell division, resulting in uncontrolled cell growth and potential spread. With over 100 types, it is a leading global cause of death, second only to cardiovascular disorders. External factors, such as smoking, diet, obesity, infection, radiation, and environmental stress, contribute to cancer development. Definitive treatment is necessary for future management as traditional methods such as surgery, chemotherapy, and radiotherapy have drawbacks such as side effects, cancer resistance, and recurrence. Angiogenesis

Access this article online

is a critical process that is required for many physiological and pathological activities.^[1,2]

Address for correspondence: Dr. Hossein Javid,
Department of Medical Laboratory Sciences, Varastegan Institute for
Medical Sciences, Mashhad 9179666769, Iran; Dr. Mehdi Karimi-Shahri,
School of Medicine, Mashhad University of Medical Sciences,
Mashhad 9179666769, Iran.
E-mail: Javidh@varastegan.ac.ir

Submission: 19-Jun-2024 Accepted: 01-Dec-2024 Published: 30-Sep-2025

This is an open access journal, and articles are distributed under the terms of the Creative Commons Attribution-NonCommercial-ShareAlike 4.0 License, which allows others to remix, tweak, and build upon the work non-commercially, as long as appropriate credit is given and the new creations are licensed under the identical terms.

For reprints contact: WKHLRPMedknow_reprints@wolterskluwer.com

How to cite this article: Al-Kariti W, Roomi AB, Amiri H, Javid H, Karimi-Shahri M. Synthesis of SLN nanoparticles containing naringenin decorated with folate-conjugated chitosan to evaluate its anticancer effects. Med J Babylon 2025;22:909-21.

Quick Response Code:

Website:
https://jour

Website: https://journals.lww.com/mjby

DOI

10.4103/MJBL.MJBL_677_24

From a medical perspective, the flavonoid naringenin (NRG) has most fascinating and important properties.[3] This hydrophobic molecule is referred to in chemistry as 2,3-dihydro-5,7-dihydroxy-2-(4-hydroxyphenyl)-4H-1benzopyran-4-one. NRG has numerous therapeutic effects, including antioxidant, anticancer, anti-inflammatory, and hepatoprotective effects. It has been tested on various cancer cell lines, including prostate cancer, breast, liver, and human melanoma.^[4] However, its clinical application is limited due to its low solubility, instability, permeability, and bioavailability. The anticancer effects of NRG were demonstrated through the induction of tumor cell death and inhibition of angiogenesis in malignant melanoma in vitro. These findings provide evidence for the potential of NRG as a safe and effective therapeutic agent for treating various cancers, including melanoma, lung cancer, prostate cancer, hepatocellular carcinoma (HepG2 cells), breast cancer, and colon cancer.[5]

Nanoscience offers unique advantages in the field of drug delivery by utilizing nanoscale carriers to enhance the drug solubility and half-life. The key objective of drug delivery platforms is to target specific tissues and optimize drug efficacy.^[6,7]

Solid lipid nanoparticles (SLNs) have shown potential as nanocarriers for cancer therapy, with the ability to be surface-modified with ligands such as transferrin and folic acid (FA) for targeting specific receptors on cancer cells. By targeting receptors that are overexpressed on tumor cells, such as folic acid receptors (FRs), the delivery of anticancer drugs can be more effective, while minimizing side effects on healthy tissues. FRs are particularly valuable targets for delivering therapeutic agents to tumor cells. [8]

Furthermore, various studies have highlighted the effectiveness of functional ligands in enhancing the specificity of drug delivery systems. The use of EGFconjugated liposomes has demonstrated specific targeting of epidermal growth factor receptor-expressing cells in vitro, showing superior efficacy compared to other binding modes.[9] Nanoparticles are then internalized through receptor-mediated endocytosis. The attachment of chitosan (CS) to the surface of nanoparticles increases the positive charge of the particles and allows them to be attached and internalized more through passive transport. FA is a small molecule with high solubility in water and stability at various temperatures and pH. It is essential for nucleotide biosynthesis and cell division. The FA receptor, attached to the plasma membrane by glycosylphosphatidylinositol, is highly expressed in cancer cells and less expressed in normal cells.[10,11] The objective of this study is to encapsulate NRG within unmodified SLNs and evaluate the surface modification of SLNs, along with their anticancer effects, in comparison to free NRG. Apoptosis and angiogenesis mechanisms were evaluated as the most important mechanisms involved in inhibiting cancer cells.

MATERIALS AND METHODS

NRG was acquired from Golexir Pars, Mashhad, Iran. The substances obtained from Sigma-Aldrich for encapsulation purposes consisted of stearic acid, acetic acid, Tween 80, lecithin, low molecular weight CS, FA, 1-ethyl-3-(3-dimethylaminopropyl) carbodiimide (EDC), and N-hydroxysuccinimide (NHS). Sigma-Aldrich also supplied 3-(4,5-dimethylthiazol-2-yl)-2,5diphenyltetrazolium bromide (MTT), dimethyl sulfoxide (DMSO), phosphate-buffered saline tablets, acridine orange (AO), propidium iodide (PI), and trypsin. Materials utilized for cell cultures, such as fetal bovine serum (FBS), penicillin, streptomycin, and Roswell Park Memorial Institute (RPMI) cell culture medium, were obtained from Gibco. The MCF-7 breast cancer cells used in the study were provided by the cell bank of the Pasteur Institute of Tehran.

Synthesis of SLN containing NRG

The study synthesized SLN nanoparticles by mixing two organic and aqueous phases. The lipid phase was prepared using 100 mL of stearic acid and 200 mg/mL of lecithin (1:2 (W/W)), while the aqueous phase was prepared using a combination of 40 mL of Tween 80 and 60 mL of deionized distilled water. About 10 mg/mL of NRG was added to the lipid phase, incubated at 80°C for 5 min, and then homogenized at 80°C for 15 min, then sonicated for 10 min using an ultrasound probe sonicator system (15 min sonicating at 310 W, 8 s on 2 s off), and finally incubated at room temperature for 24 h. The lyophilized mixture and supernatant were collected to evaluate NRG encapsulation. [12]

Preparation of CS attached to FA

The CS-FA derivative is formed by activating the carboxyl group of FA, which then covalently binds to the primary amino group of CS, resulting in conjugation. To accomplish this, 20 mg of FA was fully dissolved in a 50 mL solution of DMSO. Subsequently, NHS (100 mM) and EDC (100 mM) were added to the mixture, while continuously stirring for 1 h. The resulting byproduct, dicyclohexylurea, was then filtered out. In the next step, the resulting mixture was slowly added dropwise to a 50 mL solution of CS (in 1% acetic acid) with a pH of 4.7, under constant stirring for 24 h. To complete the process, the pH was adjusted to 9.0 by adding aqueous sodium hydroxide, followed by dialysis using phosphate buffer and deionized distilled water. The resulting precipitate was subsequently centrifuged, dialyzed, and lyophilized. To prevent decomposition of FA, all reactions were conducted in the absence of light.^[13]

Coating SLN nanoparticles containing NRG with CS-FA

SLN nanoparticles with NRG were surface-modified with CS bound to FA. CS was dissolved in 1% acetic acid, nanoparticles dispersed in deionized water, and CS-FA

solution was added. The stirrer was incubated, centrifuged, and the supernatant was collected for FA binding.

Evaluation of the NAR entrapment rate and FA binding rate to nanoparticles

Spectrophotometric absorption was used to evaluate drug encapsulation and FA binding in nanoparticles. Standard charts of NRG and FA concentrations were prepared, and 3 mL of the supernatant collected during the centrifugation in the previous section was taken in a cuvette, and the absorbance value at 286 and 290 nm wavelength was recorded with a Techocomp UV1100 spectrophotometer using the supernatant of their corresponding blank NPs as a basic correction. The percentage of drug or FA attached to nanoparticles was calculated using the formula EE% = (amount of drug or FA bound or encapsulated)/(total drug or FA) × 100%.

Characterization procedures

The particle size, hydrodynamic diameter (z-average), polydispersity index, and surface charge (ζ -potential) of AC-SCF-NPs were assessed using dynamic light scattering (DLS) with a Malvern ZetaSizer Nano ZS90 at detection angles of 90° and 25°. For the measurements, 1 mg of samples was suspended in 10 mL of deionized distilled water and sonicated. The morphological characteristics, including shape and size, of AC-SCF-NPs were determined using a Mira3 field emission scanning electron microscope (FESEM). To prepare the samples for imaging, a few drops of the dispersed NPs were sprayed onto an aluminum foil and allowed to evaporate at room temperature. Prior to examination under the microscope, the dried particles were coated with a conductive gold layer and magnified between 10,000 and 40,000 times. Fourier transform infrared (FTIR) spectroscopy was employed to analyze the structure and functional groups of the NPs.[14] A Bruker Tensor 27 IR spectrophotometer was used to record the spectra in the wavenumber range of 400–4000 cm⁻¹. To create a compact pellet for spectrum recording, 1 mg of NPs was mixed with 200 mg of potassium bromide powder using a hydraulic press. The pellet was then placed in the instrument's sensor.

Cell culture and investigation of AC-SCF-NPs toxicity effect

In this study, the MCF-7 cell line was selected as the cancer model to evaluate the potential of AC-SCF-NPs. To initiate the cell culture, MCF-7 cancer cells were seeded at a population density of approximately 8×10^4 cells/cm² in RPMI cell culture media supplemented with 10% FBS and 1% antibiotics. The cells were carefully inspected under a sterile cabinet and subsequently incubated at 37° C in an environment containing 5% carbon dioxide and 95% humidity.

Examining the cytotoxic effect of free drugs and nanoparticles on cancer and normal cells

The study involved cultured 5000 cells in three replicates and incubated for 24 h in an incubator. The cells were treated with different concentrations of substances (0, 7.8, 15.6, 31.2, 62.5, 125, 250, and 500 µg/mL), including NRG, nanoparticles without NRG, lipid nanoparticles containing NRG (NAR-SLN-NPs), and NAR-SCF-NPs. Following treatment, the cells spent 48 h in an incubator. About 20 µL of the MTT solution (5 mg/mL) and 1000 µL of DMSO were added following incubation. More live cells were represented by the purple spectrum. Cell viability was determined using the following formula: cell viability = sample absorption minus control absorption multiplied by 100.

Examining the effect of nanoparticles on the induction of apoptosis

1. AO/PI staining

To perform this investigation, the cells were separated from the culture flasks with trypsin and were made into a cell suspension and centrifuged. Next, the culture medium was emptied on the microtube and the cells transferred in a new culture medium, and a specific volume of cells was transferred to the wells of the 6-well plate containing the culture medium. After 24 h and ensuring cell attachment to the bottom of the plate, the culture medium was replaced with the treatment medium, and the cells were incubated for 48 h. After that, the treatment medium was drained, and after washing the cells with phosphate buffer, 1 μ L of acridine and 1 μ L of PI were added to each well and subjected to microscopic examination and imaging.

2. Evaluation of gene expression

The desired gene sequences were extracted from the NCBI database, and Primer Express was used for primer design. Table 1 displays the sequences of primers that were optimized for complementary DNA (cDNA) using AlleleID 6 software. Total RNA was extracted from cells using the Rx BON kit, according to the manufacturer's protocol. In order to synthesize the cDNA strand, a solution of 1 µg/mL single-stranded RNA and oligo (dt) primer of the reverse transcription enzyme was used. Real-time PCR analyses were conducted on cDNA samples via SYBR Green Master Mix (Ampliqon, Denmark) using the Bio RAD system under thermocycling conditions consisting of a heating phase for 15 min at 95°C, followed by 40 cycles at 95°C for 15 s (denaturation phase) plus 58.5°C for 30 s (extension phase). In addition, melting curve analysis was performed for each of the genes to confirm the specificity of the primers and the absence of nonspecific products. The final data were analyzed using the $2^{-\Delta\Delta Ct}$ method using GAPDH as a normalizer.

Table 1: The primer sequences of the forward and reverse sequences that used for amplifying the targeted genes

Genes	Forward	Reverse
GAPDH	TGCTGGTGCTGAGTATG	GCATGTCAGATCCAC
	TCG	AACGG
NFK.B	CCTGCTTCTGGAGGGTG	GCCGCTATATGCAGA
	ATG	GGTGT
P53	TCAGATCCTAGCGTC	GGGTGTGGAATCAAC
	GAGCCC	CCACAG

Statistical analysis

GraphPad Prism (V.8.0) was used to analyze the data, and statistical significance was determined at a P value < 0.05. To ensure reproducibility and accuracy, all experiments were performed in triplicate. The data are presented as mean \pm SD.

RESULTS

Findings from the characterization of NAR-SLN nanoparticles

DLS results showed particles with a narrow dispersion and an average diameter of 96.08 nm. Further investigation shows a hydrodynamic diameter of about 210 nm, which indicates that SLNs containing NRG have a suitable average size and a narrow size distribution for preclinical studies [Figure 1A].

The index of repulsion between particles is called surface charge or zeta potential, and if lipid particles are in the range of 20.40 mV, they are known as stable particles. In some studies, particles above 15 mV have also been reported as particles with good stability. In the Figure 1B, the nanoparticles with NRG showed a surface charge of about 15.29 mV, which shows a sufficient repulsive force to prevent.

FTIR of SLN-NAR nanoparticles

Examination of the FTIR diagram of SLNs containing NRG shows the characteristic peaks of SLN [a peak at 1724.6 (C = C stretching) and the O-H and C-H stretching peaks at 2956.2, 2917.06, and 2850.2 cm⁻¹)] with a slight shift that this can be attributed to the successful encapsulation of NRG by nanoparticles [Figure 2].

Physicochemical results of NAR.SCF.NPs nanoparticles

1. Average particle size and dispersion index

According to the results of previous investigations, particles with an average size of 10–300 nm are suitable for clinical applications. As shown in Figure 3A, particles with an actual diameter of 162.71 nm and a dispersion index of 0.17 were detected by DLS in this study. This amount of dispersion index indicates the homogeneity

of the particle size in the prepared formulation. It shows that the presence of the coating around the nanoparticles causes more uniform dispersion of nanoparticles compared to the nanoparticles without coating. In addition, the increase in the size of the particles after coating also confirms the presence of the coating around the nanoparticles.

2. Surface charge of nanoparticles

The surface charge of nanoparticles after coating was investigated similarly, and Figure 3B showed the surface-modified nanoparticles with CS. FA has a zeta potential of +24.9 mV. The increase in surface charge, along with the change in surface charge from negative to positive, indicates the improvement of the physicochemical properties of nanoparticles and the improvement of their stability after coating.

3. Morphology of NAR-SCF-NP nanoparticles

In Figure 4A, the spherical morphology and almost smooth surface of the nanoparticles were reported from FESEM microscopy results. Particle size analysis reveals that the typical particle is smaller than 200 nm, which is comparable and consistent with the results of DLS.

4. FTIR of NAR-SCF-NPs, SCF-NPs, and NAR nanoparticles

Examining the functional groups of NRG, drug-free nanoparticles and drug-containing nanoparticles show that the drug-containing nanoparticles have all peaks in the blank nanoparticles, with a slight change, in addition to the presence of some peaks related to s in the capsule-coated nanoparticles. It confirms the incorporation of the drug into CS-FA-coated SLN nanoparticles [Figure 4B].

Investigating the amount of encapsulation of NRG in nanoparticles

The extent of drug encapsulation in SLN-NAR and NAR-SCF-NP nanoparticles, according to the standard graph drawn for different concentrations of NRG, is 73.4% and 91.45%, respectively [Figure 5A]. These results indicate the role of the created coating in preserving the drug and increasing the encapsulation percentage.

Examining the degree of binding of FA to nanoparticles

The rate of binding of FA to the surface of NAR-SCF-NP nanoparticles was evaluated by spectrophotometry and was reported as 87.55%, indicating a high binding rate. In Figure 5B, the amount of absorption of different concentrations of FA at the wavelength of 290 nm is reported, and the resulting standard graph was reported with the formulation y = 0.83661x + 0.2414 and the correlation coefficient $R^2 = 0.97$.

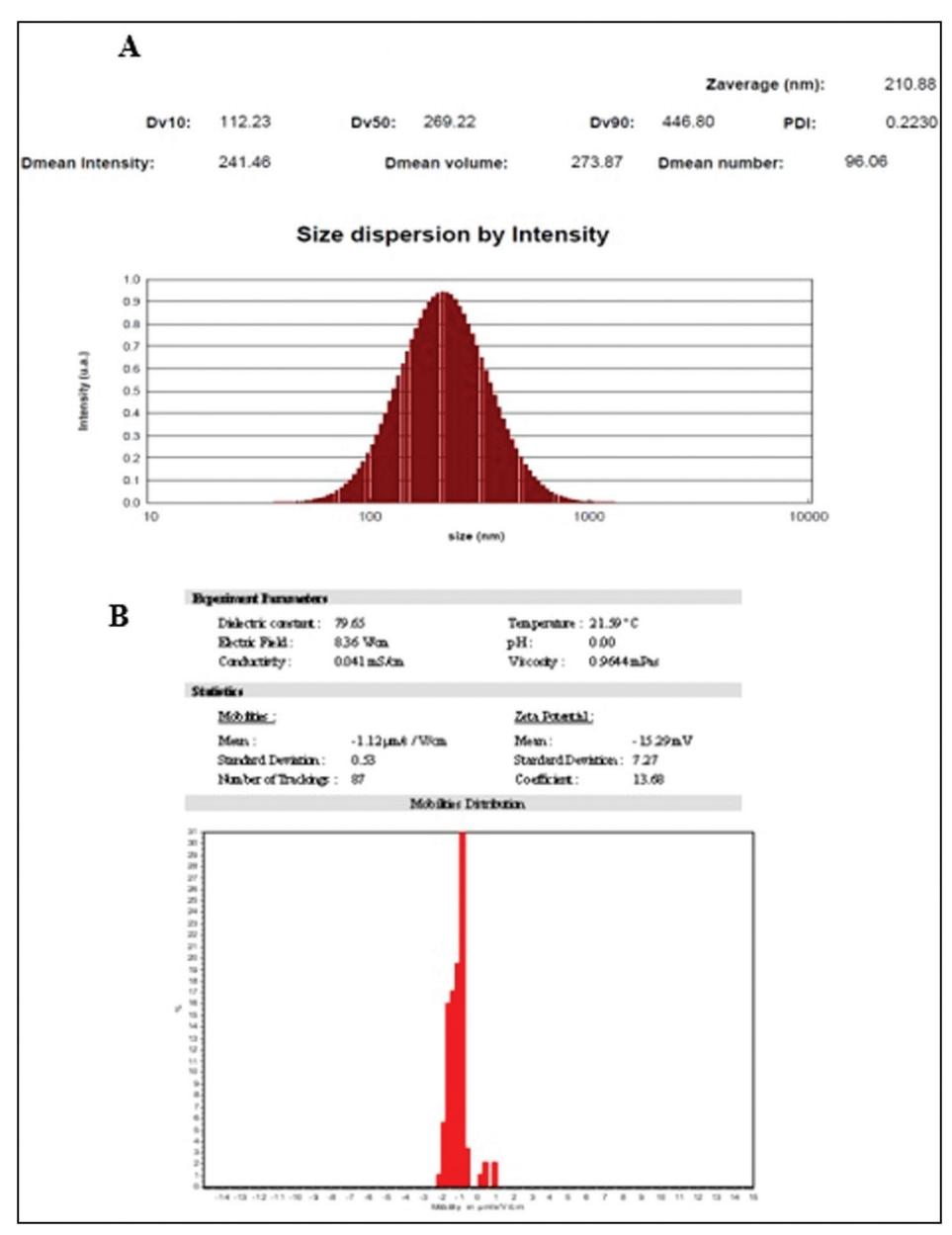


Figure 1: (A) Physicochemical characteristics and (B) surface charge of SLN-NAR nanoparticles

Toxic effect of NRG and nanoparticles

1. NRG toxicity effect on MCF-7 breast cancer cells

Assessment of the toxicity of NRGs to breast cancer cells at three time points of 24, 48, and 72 h and at different concentrations of NRG reported the absence of significant toxicity. A decrease in the cell viability has been reported during the increase in the treatment time and concentration of NRG; however, the extent of this decrease is statistically meaningless and can be ignored [Figure 6A].

2. Toxic effect of drug-free nanoparticles on cancer cells

Nanoparticles without medicinal components were tested for toxicity against breast cancer cells three times, and at concentrations ranging from 500 to 7.8 ng/mL, and were shown to be nontoxic at all three times [Figure 6B]. These results indicate the lack of toxicity of the synthesized carrier for encapsulating nanoparticles.

3. NAR-SLN toxicity effect

Investigating the toxicity of SLNs containing NRG at three time points (24, 48, and 72 h) and different concentrations against cancer cells Figure 6C showed that nanoparticles can kill cancer cells with IC_{50} values of about 183, 98, and 59 µg/mL. Liter restrain. In addition, a decrease in the cell viability was also reported during the increase in the treatment concentration. These results confirm the concentration. Also, time-dependent inhibitory effects of nanoparticle treatment on breast cancer cells were reported.

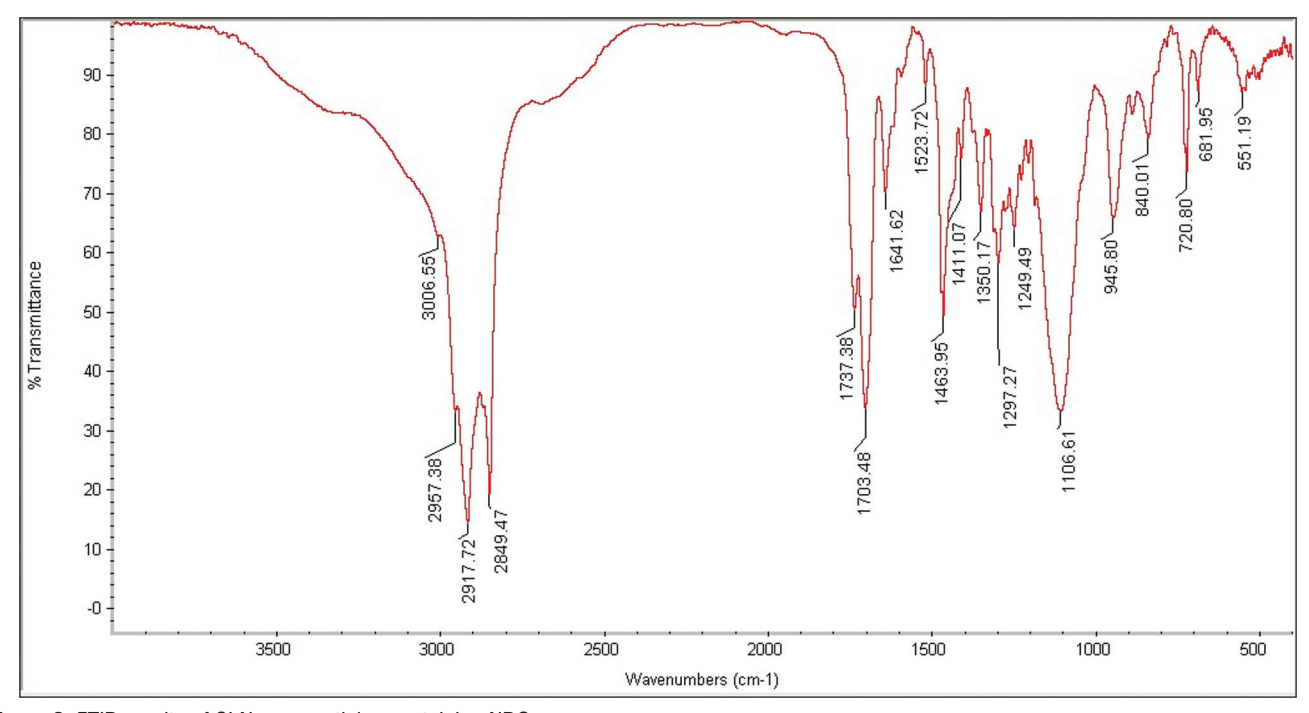


Figure 2: FTIR results of SLN nanoparticles containing NRG

4. Toxic effect of NAR-SCF-NPs on breast cancer cells

Examining the toxicity of SLNs modified with CS-FA containing drugs against breast cancer cells showed that nanoparticles with IC $_{50}$ values of about 49, 32, and 23 µg/mL are capable of inhibiting cancer cell activity at 24, 48 and 72 h of treatment [Figure 6D]. These results confirmed the time-dependent inhibitory effects of nanoparticles against cancer cells. On the other hand, the cell viability decreased with the increase in nanoparticle concentration, which indicates the effects of toxicity depending on the concentration of nanoparticles. This study's findings suggest that coating nanoparticles with CS-FA increases their uptake by cancer cells and reduces their IC $_{50}$ because the coating prevents the nanoparticles from being degraded by the cells' natural degradation processes.

5. Toxic effect of NAR-SCF-NPs on normal cells

Two-time efficiency analysis of nanoparticle toxicity on normal cells revealed that the effect of toxicity varied with nanoparticle concentration and time. When compared to the toxicity of nanoparticles on breast cancer cells, the IC $_{50}$ value for cells at 24 and 48 h was found as 496 and 267 g/mL, respectively [Figure 6E]. These findings demonstrate the tolerability of nanoparticles when used at quantities capable of killing cancer cells without harming healthy cells.

Assessment of the apoptosis power of nanoparticles

1. AO/PI staining results

Examining cells during AO/PI staining shows significant changes in terms of morphology and quantity of cells

during increasing treatment concentration. In this type of cell staining, green color shows live cells in acridine staining, while apoptotic cells show orange color in PI staining. As shown, in the control sample, all the cells are green and with elongated and elongated morphology, while in the experimental groups treated with nanoparticles, the number of cells decreased with the increase in the treatment concentration; some cells are observed in orange and with spherical morphology, which indicates the apoptotic effects depending on the concentration of nanoparticles [Figure 7].

2. Evaluation of the expression level of apoptotic genes

The nuclear factor kappa B (NFKB) gene expression in breast cancer cells treated with different concentrations of nanoparticles showed a significant decrease during the increase in treatment concentration. NFKB activates the genes responsible for cell proliferation. It inhibits apoptosis, so the decrease in its expression in the treated cells indicates an increase in the occurrence of apoptosis in the cells [Figure 8A]. Furthermore, the results of this study reported an increase in the expression of the P53 gene in cells treated with nanoparticles, which indicates the role of nanoparticles in inducing apoptosis [Figure 8B].

DISCUSSION

Chemotherapy drug application is limited in terms of stability, solubility, and toxicity for healthy cells, as well as side effects such as hair loss and loss of appetite. Herbal agents have long been considered promising candidates for the development of anticancer drugs. Herbal compounds

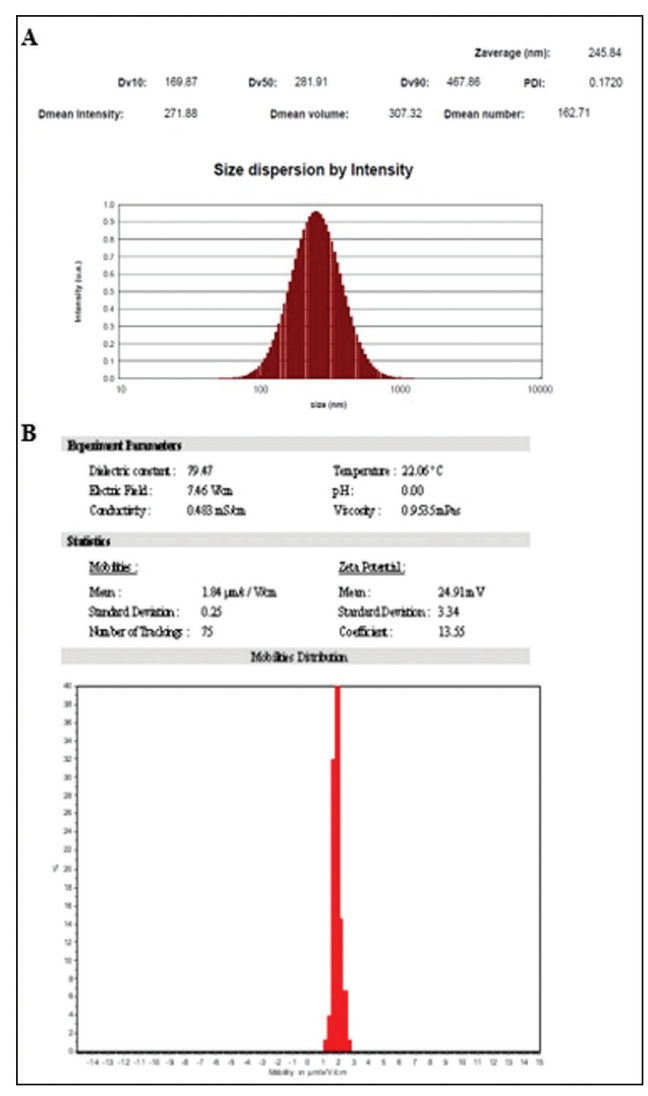


Figure 3: (A) DLS results including average particle size and polydispersity index and (B) zeta potential diagram of NAR-SCF-NP nanoparticles

have been shown to inhibit cancer cell survival and invasion by affecting various signaling pathways, including the PI3K/Akt pathway, the Wnt/ β -catenin signaling pathway, the vascular endothelial growth factor pathway, and the mitogen-activated protein kinase cascade. [15]

Plant compounds, such as flavonoids like NRG, offer a potential alternative for cancer treatment with minimal side effects. [16] NRG exhibits anticancer properties by inhibiting cancer cell growth and inducing cell death in various types of cancer. It also has anti-inflammatory, antioxidant, and antibacterial activities, making it a promising candidate for further research and development in cancer therapy. [17] NRG's limited bioavailability due to its hydrophobic nature can be addressed through application of nanoscale delivery systems. Nanocarriers, such as polymer-based, lipid-based, micelle-based, protein-based, and carbon-based nanoparticles, provide a protective coating that enhances

the bioavailability, enables targeted delivery, and improves the stability and solubility of NRG.[18] These nanocarriers offer advantages like high surface-to-volume ratio and resistance to degradation, allowing for efficient drug delivery and manipulation of pharmacological properties. Numerous studies have focused on utilizing nanocarrierbased delivery systems to enhance the bioavailability and stability of NRG.[19] This is the first study to explore the effects of NRG, a flavonoid compound with anticancer capabilities, on the activation of the apoptotic pathway after loading SLN nanoparticles modified with CS for FA binding. It enables the development of a targeted drug delivery system for cancer treatment. By incorporating NRG into SLNs and decorating them with FA-conjugated CS, the nanoparticles can specifically target cancer cells while minimizing damage to healthy cells. Evaluating the anticancer effects of these nanoparticles provides valuable insights into their potential efficacy, mechanism of action, and potential for clinical application in improving cancer treatment outcomes.

In order to circumvent the problems inherent in more traditional drug formulations, researchers have been focusing on lipid-based drug delivery for the past 2 decades. This is especially true in areas with limited access to clean water-liquid medications.[20] Carrier lipids, which can be amphipathic or hydrophobic, transport active chemicals throughout the body. Lipid nanoparticle drug delivery methods have been around since the early nineteenth century, when a German scientist named R.H. Müller and an Italian professor named M. Gascon created them.[20] Only solid lipids or a combination of solid and liquid lipids can be used to create lipid nanoparticles.[20] Free fatty acids, fatty alcohols, triglycerides, steroids, and waxes are all examples of lipids that make up nanoparticles, [20] and glycolipids, phospholipids, and sphingolipids are also included.[21] Because of their high drug solubility, controlled release, low toxicity, and biodegradability, lipid particles are widely used in drug delivery. The most important characteristics of synthesized lipid nanoparticles are their size, zeta potential, crystallinity rate, polymorphism, drug loading, and drug release. In the past, NRG has been encapsulated in SLNs, nanostructured lipid carriers (NLCs), and liposomal formulations. [20]

Nanoparticle modification effectively entraps pharmaceuticals, suppressing adverse effects by increasing the drug concentration, decreasing the effective dose, and controlling undesired symptoms. This study attached FA to nanoparticles for delivery to breast cancer cells, using CS to increase the efficiency and half-life, [22] FA. Multiple studies have demonstrated the utility of Arg-Gly-Asp (RGD) in the selective targeting and delivery of anticancer medicines to cancer cells. Several techniques were used to detect nanoparticles in this study, including DLS, scanning electron microscopy, and FTIR spectroscopy, and the results

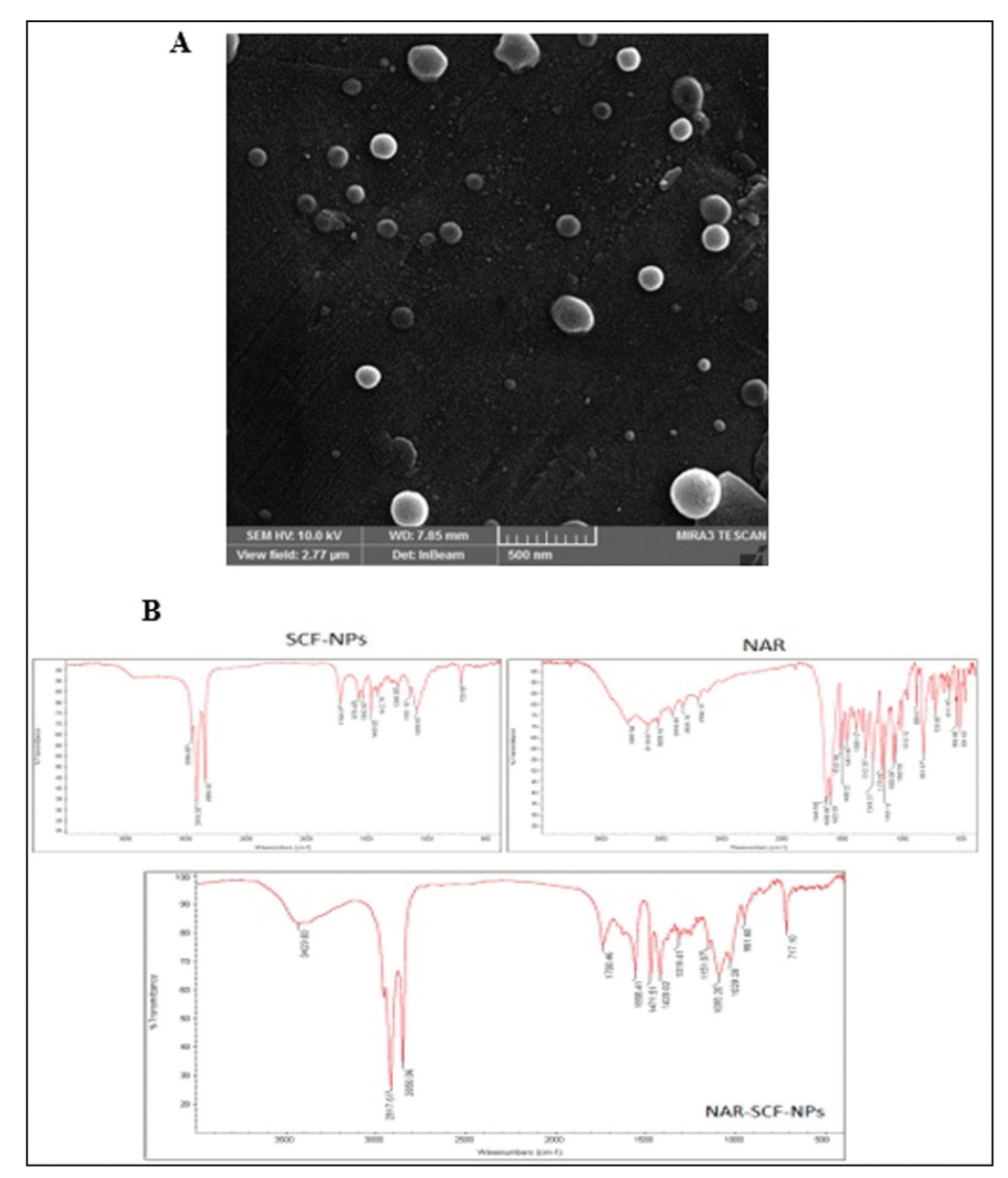


Figure 4: (A) Field emission scanning electron microscopy images of NAR-SCF-NP nanoparticles and (B) FTIR diagram of NRG (NAR), blank nanoparticles (SCF-NPs), and CS-FA modified nanoparticles containing NRG (NAR-SCF-NPs)

indicated the creation of nanoparticles with suitable dimensions (162.71 nm) to flee the reticuloendothelial system. [23] Similar experiments have been undertaken to encapsulate NRG in various nanoparticles to boost its bioavailability and therapeutic effects, as seen in the current work. Nanocrystals of NRG were created in a study in 2018, for example, and they had dimensions of 349.2 nm, a dispersion index of 0.23, a surface charge of 13.86 mV, and a rod-like shape with a smooth surface. In a study with methods comparable to the present one, the drug loading efficiency was reported to be 88.16%. Uniformly dispersed, 88 nm in size, zeta potential of 15.36 mV NRG-loaded CS nanoparticles were produced in a study performed in 2019. The NRG loading rate was found to be over 91% in this study. [24]

SLNs was first introduced in 1991. When solid lipids are stabilized by emulsifiers, they form SLNs, the first lipid nanoparticles.^[20] Sub-micron sized (1000 nm) SLNs are extremely small. The benefits of liposomes and emulsions over polymers include lower toxicity, regulated drug release, decreased chemical degradation, and reduced cost. However, their unstable crystal structure and low solubility in drugs are drawbacks.^[25]

In 2016, researchers developed an NRG delivery system using SLN nanoparticles to improve the stability, enhance pulmonary bioavailability, and control drug release. The system, loaded with NRG via low-temperature emulsification and freezing, showed no toxicity and

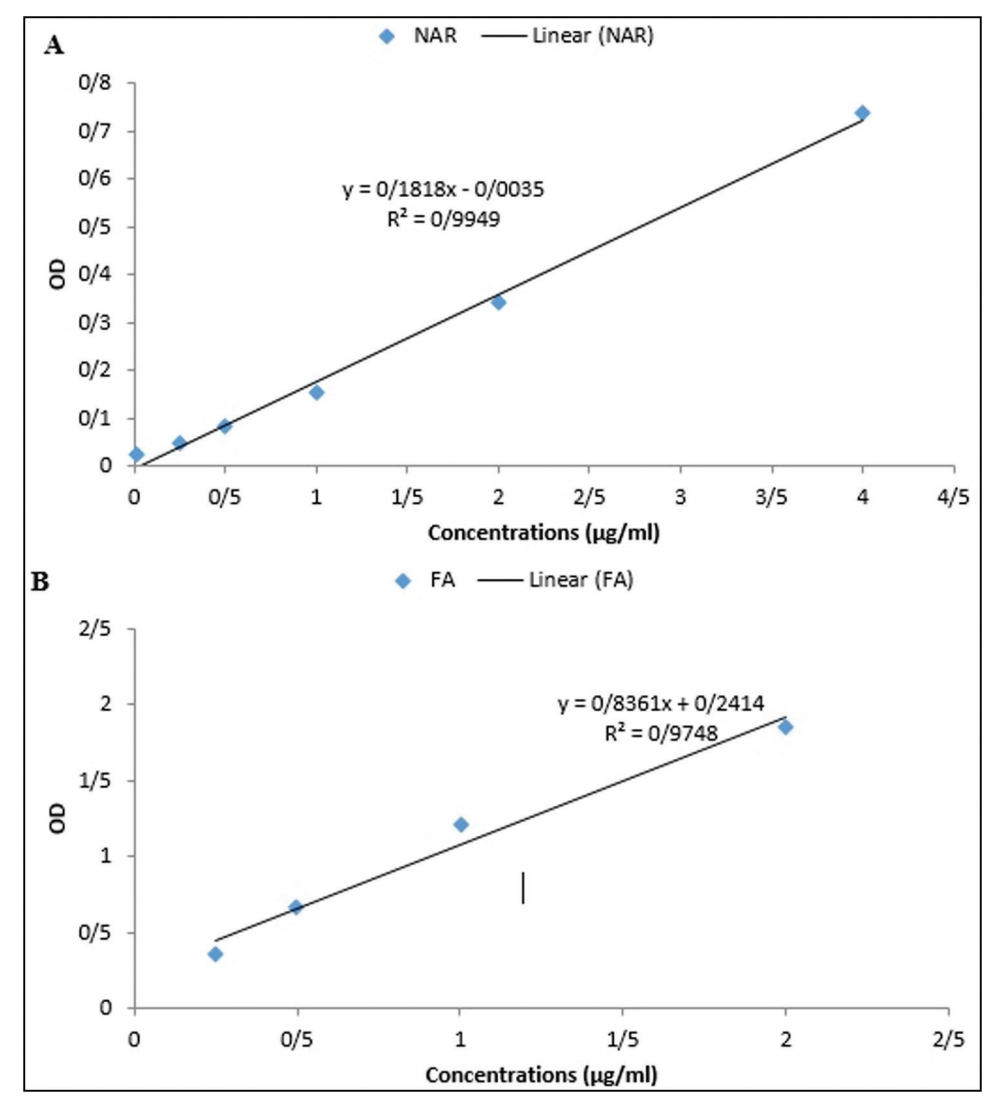


Figure 5: (A) The standard graph obtained from different concentrations of NRG at a wavelength of 286 nm and (B) the standard graph obtained from different concentrations of FA at a wavelength of 290 nm

increased bioavailability when administered via the lungs. [26]

In a separate investigation, the combination of oxaliplatin and NRG-loaded NLCs was tested for its ability to induce apoptosis in colon cancer cells (HT.29).[27] Seven years after the discovery and synthesis of the first generation of lipid-based nanoparticles, SLNs, NLCs were discovered and produced.[21] NLCs, which are composed of both solid and liquid lipids, have a greater capacity to encapsulate pharmaceuticals compared to SLNs. They have the potential to improve medication solubility in the lipid matrix and provide finer regulation of drug release. Because of their small size, they also have a lower explosive potential.^[28] In a study published in 2019, researchers used heat homogenization to encapsulate NRG in NLCs. Nanoparticles ranged in size from 50 nm up to 120 nm (average size = 98). The MTT assay and DAPI staining were used to determine the cytotoxicity of nanoparticles. When cells were incubated for 24 h, the results demonstrated that the toxicity of NRG-NLCs was remarkably similar to that of NRG alone in limiting cell growth. When NRG was used to induce apoptosis in colonic HT-29 cells, flow cytometry revealed an increase in the number of apoptotic cells of NRG-NLCs. Real-time PCR data also showed that the expression of anti-apoptotic markers was downregulated, while that of pro-apoptotic Bid mRNA was upregulated. This study shows that HT-29 colon cancer cell proliferation can be inhibited by NRG loaded in NLCs. Apoptosis is induced, and anticancer treatments are more effective when combined with NRG-NLCs, and chemotherapy is less toxic.^[27]

Wang *et al.*^[29] studied how injecting NRG into liposomes changed its properties when taken orally. Thin-film hydration was used to create NRG-containing liposomes. High zeta potential values and evidence of physical stability were found. Three relevant *in vitro* digestion settings

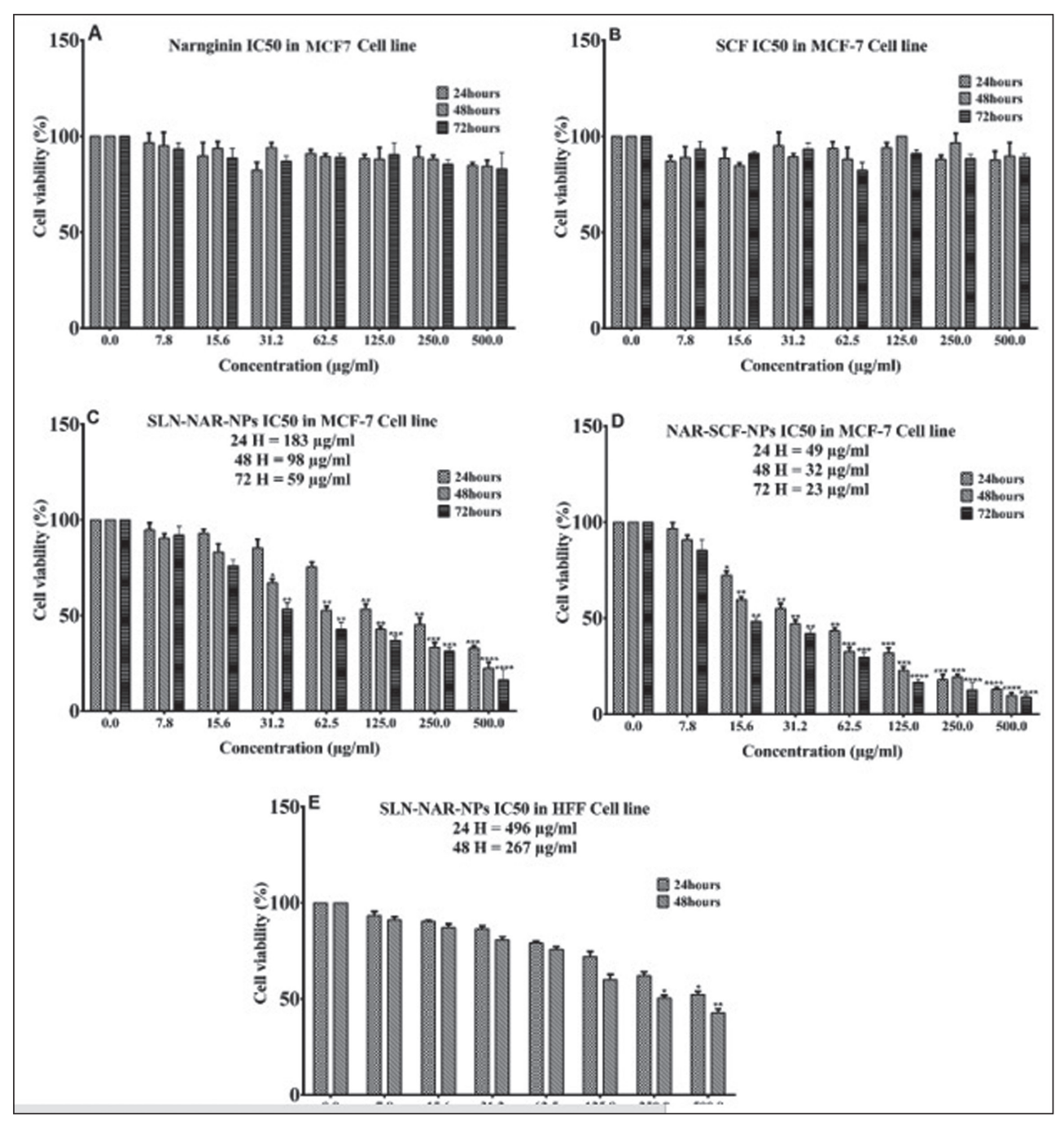


Figure 6: (A) The effect of NRG toxicity, (B) nanoparticles without NRG, (C) lipid nanoparticles containing NRG (NAR-SLN-NPs), (D) NAR-SCF-NPs on breast cancer cells in three-time efficiency and different concentrations, and (E) toxic effect of NAR-SCF-NP nanoparticles on normal cells in two-time efficiency and different concentrations. Significant differences are indicated as *P < 0.05, *P < 0.01, *P < 0.001, and *P < 0.001.

were used to derive release profiles. Analysis of tissue distribution showed that when liposomes were utilized, the NRG drug concentration was increased in a number of tissues, most notably the liver. When the encapsulated medication was given orally to rats, its solubility and oral bioavailability both increased significantly. These findings support the use of NRG-containing liposomes as a clinically viable drug delivery technology as they improve drug bioavailability and solubility.^[29]

It is clear that the physicochemical properties and drug loading in various carriers vary with the kind of carrier, the materials utilized, the technique of synthesis, etc. The present study used MTT, fluorescence staining, and quantitative polymerase chain reaction to determine whether or not SLN-FA-NPs containing NRG had an anticancer effect on FR-positive MCF-7 cancer cells. The results indicated that SLN-CS-FA-NRG-NPs at a density of 24 mcg/mL inhibited the activity of 50% of cancer cells,

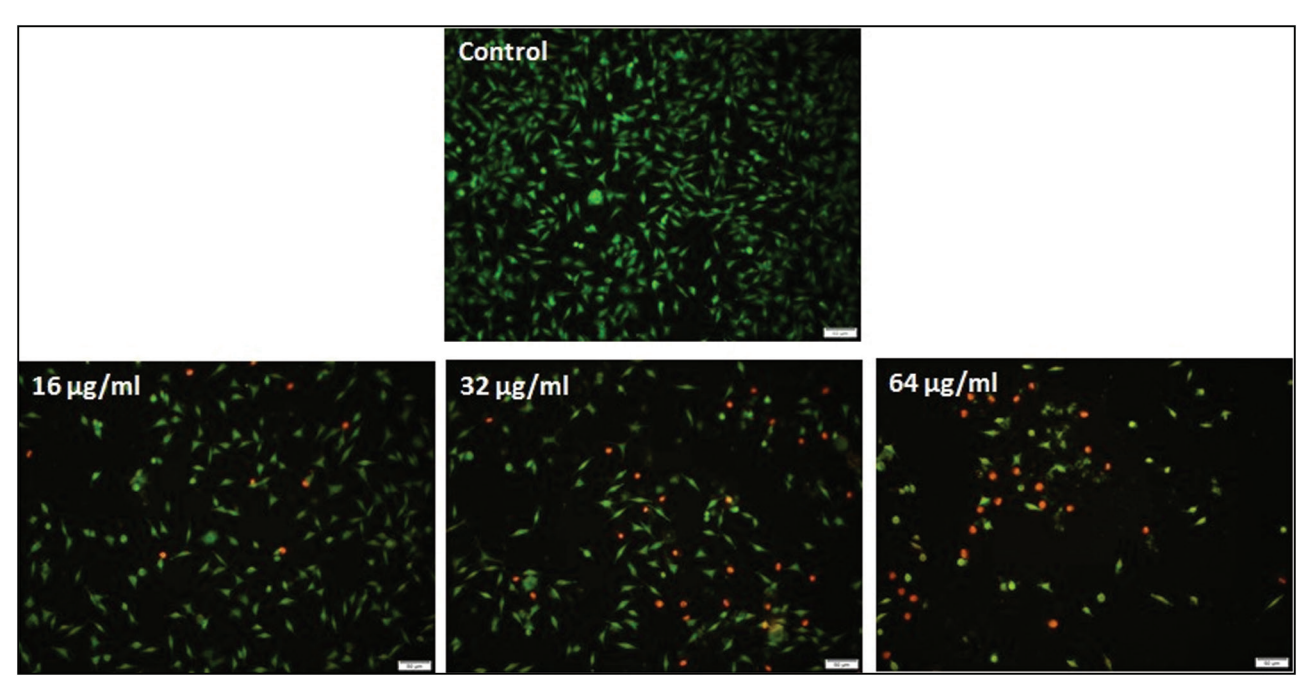


Figure 7: Acridine orange/propidium iodide staining; color change of cells from green to orange during increasing concentration of nanoparticle treatment in MCF-7 cells

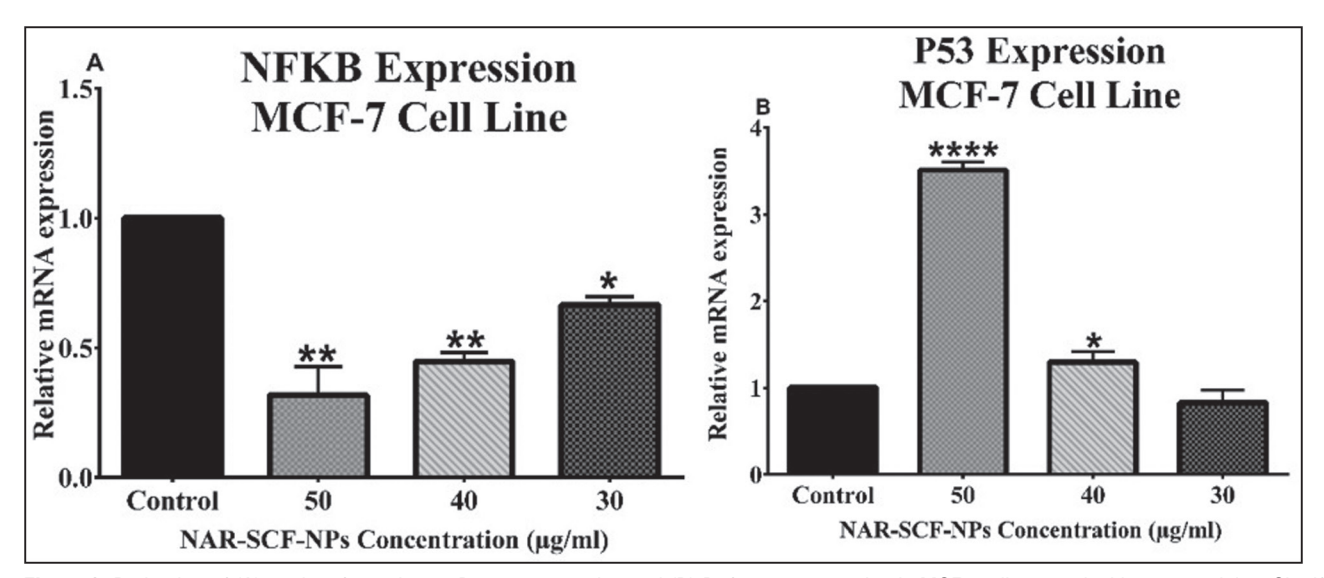


Figure 8: Reduction of (A) nuclear factor kappa B gene expression and (B) P53 gene expression in MCF7 cells treated with nanoparticles. Significant differences are indicated as *P < 0.05, **P < 0.01, and ****P < 0.0001.

while having no effect on normal cells at this concentration. Gene expression changes provided more evidence for the pro-apoptotic effects of SLN-CS-FA-NRG-NPs.

AO/PI staining indicates considerable cell morphology and quantity changes with increasing treatment. As results indicate, in the experimental groups treated with nanoparticles, the number of cells decreased with the increase in the treatment concentration, and some cells were orange and spherical, indicating apoptotic effects. Several studies have demonstrated the apoptotic effects of NRG nanoparticles on different types of cancer cells.

Zhao *et al.*^[30] found that NRG inhibited the proliferation rate of breast cancer cells and induced apoptotic cell death, as evidenced by AO/EB staining and Annexin V/PI staining. Mani *et al.*^[31] observed that proanthocyanidin (PAC)-AgNPs, which are nanoparticles containing NRG, induced apoptosis in colon cancer cells, and NRG-loaded nanoparticles increased cytotoxicity and internalization of NRG in breast cancer cells, leading to apoptosis. Furthermore, Wadhwa *et al.*^[32] demonstrated that NRG-loaded liquid crystalline nanoparticles (LCNs) induced apoptosis in lung cancer cells, as revealed by AO/EB staining.

The study found that nanoparticles led to an upregulation of the P53 gene expression and a downregulation of the NFKB gene expression in treated cells, suggesting nanoparticles play a role in triggering apoptosis. NRG nanoparticles have the potential to induce apoptosis in cancer cells through various pathways, making them a promising candidate for cancer therapy. First, NRG-loaded CS nanoparticles (CS-NPs/ NAR) increase oxidative stress, leading to the activation of pro-caspase3 and subsequent apoptosis in breast cancer cells. Second, NRG triggers intracellular reactive oxygen species (ROS) production, inhibits JAK-2/STAT-3 signaling pathways, and activates caspase-3, resulting in apoptosis in hepatocarcinoma cells.[33] Third, NRG induces intracellular ROS production and endoplasmic reticulum stress and alters the balance between apoptosis and autophagy, leading to programmed cell death in oral squamous cell carcinoma cells.[34] Lastly, NRG-loaded LCNs exhibit antiproliferative, anti-migratory, and ant colony formation activities in lung cancer cells, ultimately inducing apoptosis.[35]

CONCLUSION

Synthesis of NRG-containing SLN nanoparticles and surface modification of nanoparticles with CS were reported as successful in this study. FA by expanding particle size distribution and flipping the surface charge to the positive. These results showed an increase in the toxicity effect of NRG in the form encapsulated in nanoparticles compared to the free form. Moreover, the higher toxicity effect of surface-modified nanoparticles compared to nanoparticles without surface modification confirmed the role of CS-FA coating in the internalization of nanoparticles to cancer cells.

Acknowledgments

We would like to appreciate the cooperation of all those whose medical records were used in this study and their families.

Author contributions

Wurood Al-Kariti, Ali B. Roomi, Hamed Amiri, and Hossein Javid conceived and planned the experiments and was involved in the management of the cases. Hossein Javid and Wurood Al-Kariti carried out the experiments. Ali B. Roomi analyzed the data. Hamed Amiri and Hossein Javid wrote the initial manuscript. Mehdi Karimi-Shahri and Hossein Javid assisted in writing the revised manuscript. All authors approved the final version for submission.

Data availability

The authors of this article will share all the data underlying the findings of their manuscripts with other researchers. Therefore, I hereby declare the statement of "availability" for the data used in this manuscript. researchers can communicate with the first author and the corresponding authors for the data by email.

Financial support and sponsorship

Nil.

Conflicts of interest

There are no conflicts of interest.

REFERENCES

- 1. Folkman J. Angiogenesis. Annu Rev Med 2006;57:1-18.
- Saleh RH, Khalaf AA. The antimicrobial activity of nanochitosan and nano-CaCO. Med J Babylon 2023;20:540-6.
- Nouri Z, Fakhri S, El-Senduny FF, Sanadgol N, Abd-ElGhani GE, Farzaei MH, et al. On the neuroprotective effects of naringenin: Pharmacological targets, signaling pathways, molecular mechanisms, and clinical perspective. Biomolecules 2019;9:690.
- Choi J, Lee D-H, Jang H, Park S-Y, Seol J-W. Naringenin exerts anticancer effects by inducing tumor cell death and inhibiting angiogenesis in malignant melanoma. Int J Med Sci 2020;17:3049-57.
- Fadholly A, Ansori AN, Utomo B. Anticancer effect of naringin on human colon cancer (widr cells): In vitro study. Res J Pharmacy Technol 2022;15:885-8.
- Haghighi AA, Ramezani M, Hashemnia A, Malekzadeh A. Synthesis and characterization of multifunctional graphene oxide with gamma-cyclodextrin and SPION as new nanocarriers for drug delivery. Appl Chem Today 2019;14:35-50.
- Jasim RA. Medical, pharmaceutical, and biomedical applications of chitosan: A review. Med J Babylon 2021;18:291-4.
- Einafshar E, Javid H, Amiri H, Akbari-Zadeh H, Hashemy SI. Curcumin loaded β-cyclodextrin-magnetic graphene oxide nanoparticles decorated with folic acid receptors as a new theranostic agent to improve prostate cancer treatment. Carbohydr Polym 2024;340:122328.
- Skóra B, Szychowski KA. Molecular mechanism of the uptake and toxicity of EGF-LipoAgNPs in EGFR-overexpressing cancer cells. Biomed Pharmacother 2022;150:113085.
- Amiri H, Javid H, Einafshar E, Ghavidel F, Rajabian A, Hashemy SI, et al. Development and evaluation of PLGA nanoparticles surfaced modified with chitosan-folic acid for improved delivery of resveratrol to prostate cancer cells. BioNanoScience 2024;14:988-98.
- Khorramdel M, Ghadikolaii FP, Hashemy SI, Javid H, Tabrizi MH. Nanoformulated meloxicam and rifampin: Inhibiting quorum sensing and biofilm formation in *Pseudomonas aeruginosa*. Nanomedicine 2024;19:615-32.
- Baek J-S, Pham CV, Myung C-S, Cho C-W. Tadalafil-loaded nanostructured lipid carriers using permeation enhancers. Int J Pharm 2015;495:701-9.
- Naghibi Beidokhti HR, Ghaffarzadegan R, Mirzakhanlouei S, Ghazizadeh L, Dorkoosh FA. Preparation, characterization, and optimization of folic acid-chitosan-methotrexate core-shell nanoparticles by Box-Behnken design for tumor-targeted drug delivery. Aaps Pharmscitech 2017;18:115-29.
- Einafshar E, Einafshar N, Khazaei M. Recent advances in MXene quantum dots: A platform with unique properties for generalpurpose functional materials with novel biomedical applications. Top Curr Chem (Cham) 2023;381:27.
- Einafshar E, Mobasheri L, Hasanpour M, Rashidi R, Ghorbani A. Pro-apoptotic effect of chloroform fraction of *Moraea* sisyrinchium bulb against glioblastoma cells. Biomed Pharmacother 2024;170:115931.
- Nema R, Khare S, Jain P, Pradhan A, Gupta A, Singh D. Natural products potential and scope for modern cancer research. Am J Plant Sci 2013;4:1270-7.
- Kumar R, Bhan Tiku A. Naringenin suppresses chemically induced skin cancer in two-stage skin carcinogenesis mouse model. Nutr Cancer 2020;72:976-83.
- Hosny KM, Alharbi WS, Almehmady AM, Bakhaidar RB, Alkhalidi HM, Sindi AM, et al. Preparation and optimization of pravastatin-naringenin nanotransfersomes to enhance

- bioavailability and reduce hepatic side effects. J Drug Delivery Sci Technol 2020;57:101746.
- Bhia M, Motallebi M, Abadi B, Zarepour A, Pereira-Silva M, Saremnejad F, et al. Naringenin nano-delivery systems and their therapeutic applications. Pharmaceutics 2021;13:291.
- Mohammadi-Samani S, Masoumzadeh P, Ghasemiyeh P, Alipour S. Oxybutynin-nanoemulgel formulation as a successful skin permeation strategy: In-vitro and ex-vivo evaluation. Front Mater 2022;9:848629.
- Gordillo-Galeano A, Mora-Huertas CE. Solid lipid nanoparticles and nanostructured lipid carriers: A review emphasizing on particle structure and drug release. Eur J Pharm Biopharm 2018:133:285-308.
- Soe ZC, Kwon JB, Thapa RK, Ou W, Nguyen HT, Gautam M, et al. Transferrin-conjugated polymeric nanoparticle for receptor-mediated delivery of doxorubicin in doxorubicin-resistant breast cancer cells. Pharmaceutics 2019;11:63.
- Gu L, Shi T, Sun Y, You C, Wang S, Wen G, et al. Folate-modified, indocyanine green-loaded lipid-polymer hybrid nanoparticles for targeted delivery of cisplatin. J Biomater Sci Polym Ed 2017;28:690-702.
- Md S, Alhakamy NA, Aldawsari HM, Asfour HZ. Neuroprotective and antioxidant effect of naringenin-loaded nanoparticles for noseto-brain delivery. Brain Sci 2019:9:275.
- Patri AK, Kukowska-Latallo JF, Baker JR. Targeted drug delivery with dendrimers: Comparison of the release kinetics of covalently conjugated drug and non-covalent drug inclusion complex. Adv Drug Deliv Rev 2005;57:2203-14.
- Park S, Lim W, Bazer FW, Song G. Naringenin induces mitochondria-mediated apoptosis and endoplasmic reticulum stress by regulating MAPK and AKT signal transduction pathways in endometriosis cells. Mol Hum Reprod 2017;23:842-54.

- Raeisi S, Chavoshi H, Mohammadi M, Ghorbani M, Sabzichi M, Ramezani F. Naringenin-loaded nano-structured lipid carrier fortifies oxaliplatin-dependent apoptosis in HT-29 cell line. Process Biochem 2019;83:168-75.
- Hosseini H, Jafari SM. Introducing nano/microencapsulated bioactive ingredients for extending the shelf-life of food products. Adv Colloid Interface Sci 2020;282:102210.
- Wang F, Li L, Liu B, Chen Z, Li C. Hyaluronic acid decorated pluronic P85 solid lipid nanoparticles as a potential carrier to overcome multidrug resistance in cervical and breast cancer. Biomed Pharmacother 2017;86:595-604.
- Zhao Z, Jin G, Ge Y, Guo Z. Naringenin inhibits migration of breast cancer cells via inflammatory and apoptosis cell signaling pathways. Inflammopharmacology 2019;27:1021-36.
- Mani S, Balasubramanian MG, Ponnusamy P, Vijayan P. Antineoplastic effect of PAC capped silver nanoparticles promote apoptosis in HT-29 human colon cancer cells. J Cluster Sci 2019;30:483-93.
- 32. Wadhwa R, Paudel KR, Chin LH, Hon CM, Madheswaran T, Gupta G, et al. Anti-inflammatory and anticancer activities of Naringenin-loaded liquid crystalline nanoparticles in vitro. J Food Biochem 2021;45:e13572.
- Zhang M, Lai J, Wu Q, Lai J, Su J, Zhu B, et al. Naringenin induces HepG2 cell apoptosis via ROS-mediated JAK-2/STAT-3 signaling pathways. Molecules 2023;28:4506.
- 34. Ji P, Yu T, Liu Y, Jiang J, Xu J, Zhao Y, *et al.* Naringenin-loaded solid lipid nanoparticles: Preparation, controlled delivery, cellular uptake, and pulmonary pharmacokinetics. Drug Des Dev Ther 2016;10:911-25.
- 35. Motallebi M, Bhia M, Rajani HF, Bhia I, Tabarraei H, Mohammadkhani N, *et al.* Naringenin: A potential flavonoid phytochemical for cancer therapy. Life Sci 2022;305:120752.